

# Corrosion Behavior of Rust DH36 Offshore Platform Steel in Seawater

J. G. Liu<sup>1</sup>, Z. L. Li<sup>1</sup>, Y. T. Li<sup>2</sup> and B. R. Hou<sup>2</sup>

<sup>1</sup> *Qingdao Key Laboratory of Circle Sea Oil & Gas Storage and Transportation Technology, College of pipeline and civil Engineering, China University of Petroleum, Qingdao, China*

<sup>2</sup> *Institute of Oceanology, Chinese Academy of Sciences, Qingdao, China*

Correspondence should be addressed to J. G. Liu: [jgliu83@163.com](mailto:jgliu83@163.com)

## Abstract

The metals exposed in offshore environment would suffer from serious corrosion. Rusts were formed with the DH36 steel immersing in the seawater for different days. Then the corrosion behavior of the rust steels was studied using polarization curves and electrochemical impedance spectroscopy. The corrosion morphologies and corrosion products of the rust samples were characterized by scanning electron microscopy and X-ray diffraction. The inner layer of the rust steel was bent flaky while the outer layer was packing flaky with cracks. The product identified in the inner layer was cementite mainly while the outer layer was lepidocrocite mainly. With metal dissolved, cementite, detected in inner rust, left on the metal and formed the no protective inner layer and lead to increasing corrosion rate in the test time.

**Keywords:** marine corrosion; rust; cementite

## Introduction

With the development of ocean resources, steel structures, such as offshore oil platforms, dolphin, are constructed and put used in marine environment. The offshore environment is one of the most corrosive natural occurring environments. Corrosion of steel structures in marine environment is a big problem that has to be considered [1–10]. Due to the complexity of the marine environment, steel structures exposed to this environment will seriously corrode [11–19]. Not only the simple electrochemical corrosion, but also electrochemical and mechanical function corrosion, biological corrosion would happen in this area.

Because of the complexity of the seawater, it is still a subject of great interest to know the corrosion behavior of DH36 steel. The DH36 steel shows good mechanical properties and

corrosion resistance, and it is commonly used for offshore oil platform in China. However, literature revealed that studies have not been made so far about the use of DH36 steel for offshore oil platform exposed in marine environment. The corrosion process of DH36 steel in seawater was studied using electrochemical tests while the morphologies and rusts of the steel samples were characterized by scanning electron microscopy (SEM) and X-ray diffraction (XRD).

## **Materials and Methods**

### **Specimens**

DH36 steel was used with chemical compositions (in wt-%) of 0.15C, 0.33Si, 1.40Mn, 0.015P, 0.005S, 0.06Cr, 0.07Ni, 0.15Cu, 0.035Al and balance Fe. The material was machined into size of 10 mm in diameter and left 0.7854 cm<sup>2</sup> work area. And it cut into test specimens of size 20 mm×20 mm×12 mm for rusts characterization. The specimens were wet ground down to the 1200 grit and cleaned with distilled water, ethanol and acetone [20]. Then they were immersed into Qingdao seawater for 30 days, 90 days and 180 days respectively. After removed, they were used for the tests.

### **Electrochemical tests**

The electrochemical test was measured with 2273 Potentiostat used and performed in a typical three-electrode cell. The working electrode was the rusted steel after immersion. Pt counter electrode and a saturated calomel reference electrode were used. Electrochemical impedance spectroscopy (EIS) measurement was performed in the frequency range of 100 kHz to 10 mHz, with a sinusoidal potential signal of 10 mV around the open circuit potential[21, 22]. The scan rate of polarization curves were 0.5 mV/s and the range was OCP –200 to +200mV [14].

### **Characterization of rust samples**

The images of outer and inner rust layers were characterized with scanning electron microscopy (SEM) [23, 24]. The corrosion products of the rust samples were characterized by X-ray diffraction. The XRD conditions were 6kW intensity using a Cu target [22, 25].

## Results and discussion

### Electrochemical behaviour

Figure 1 shows the polarization curves of DH36 rust steels in seawater of 30 days, 90 days and 180 days. The fitting results are shown in Table 1.

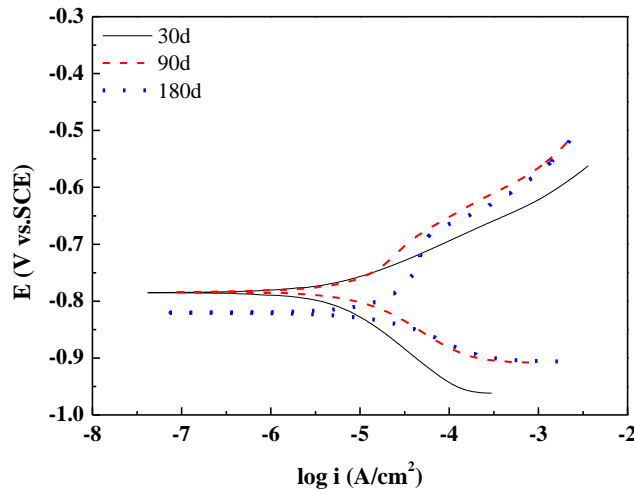


Figure 1: Polarization curves of DH36 rust steels in seawater

Table 1: Fitting parameters of polarization curves

	$E_{corr}$ (mV)	$I_{corr}$ ( $\mu\text{A}/\text{cm}^2$ )	$\beta_c$ (mV)	$\beta_a$ (mV)
30 day	-785.4	5.24	127.99	70.89
90 day	-782.6	16.37	125.64	238.54
180 day	-821.2	34.20	91.39	601.44

From the polarization curves, the corrosion current density of DH36 rust steels in seawater increased with time. As the immersion time was not enough, there was no perfect protect rust layer on the metal, corrosion rate kept increasing in 180 days. The anodic Tafel parameters ( $\beta_a$ ) increased while cathodic Tafel parameters ( $\beta_c$ ) decreased with time in 180 days. It means that corrosion of the rust steel was controlled by anodic reaction gradually with time.

Figure 2 shows the EIS and the fitting curves of DH36 rust steels in seawater and the fitting parameters are shown in Table 2. The equivalent circuit of  $R_s(C_{out}R_{out})(C_{in}(R_{in}(Q(R_{ct}Z_W))))$  was used for rust steel in seawater.  $R_s$  is the resistance of the solution,  $R_{out}$ ,  $C_{out}$  and  $R_{in}$ ,  $C_{in}$  are the resistance and capacitance of outer and inner rust layer,  $Q$  is CPE parameter,  $R_{ct}$  is charge transfer resistance,  $Z_W$  is Warburg diffusion impedance. If the rust layer grows

uniformly, the resistance increases and capacitance decreases, in proportion to the increase in thickness [26].

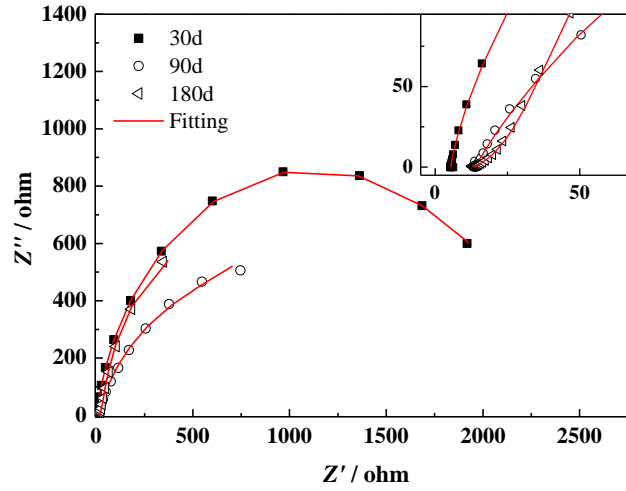


Figure 2: EIS of DH36 rust steels in seawater

Table 2: EIS fitting parameters of rust steels

	$C_{in}$ ( $F \cdot cm^{-2}$ )	$R_{in}$ ( $ohm \cdot cm^2$ )	$Q$		$R_{ct}$ ( $ohm \cdot cm^2$ )	$W$ ( $S \cdot cm^{-2} \cdot s^{-1/2}$ )	$C_{out}$ ( $F \cdot cm^{-2}$ )	$R_{out}$ ( $ohm \cdot cm^2$ )
			$Y_0$ ( $S \cdot cm^{-2} \cdot s^{-n}$ )	$n$				
30 day	$7.03 \times 10^{-4}$	7.50	0.0006632	0.6871	2233	$2.94 \times 10^{-2}$	$5.29 \times 10^{-12}$	5.412
90 day	$9.07 \times 10^{-4}$	18.22	0.003354	0.7239	2317	$5.01 \times 10^{15}$	$7.19 \times 10^{-13}$	13.51
180 day	$1.36 \times 10^{-3}$	6.24	0.01388	0.8239	2406	$6.27 \times 10^9$	$1.11 \times 10^{-14}$	13.67

From Table 2, the capacitance of the outer rust layer of DH36 rust steel decreased and the resistance increased with time, it means the thickness of the outer layer increased with time in 180 days. The change of the inner layer showed different behavior, the capacitance increased while the resistance increased at first and then decreased, this means the inner rust was complex in both composition and morphology.

## Characterization

Figure 3 and Figure 4 show the micrographs and XRD patterns of the DH36 rust steels in seawater.

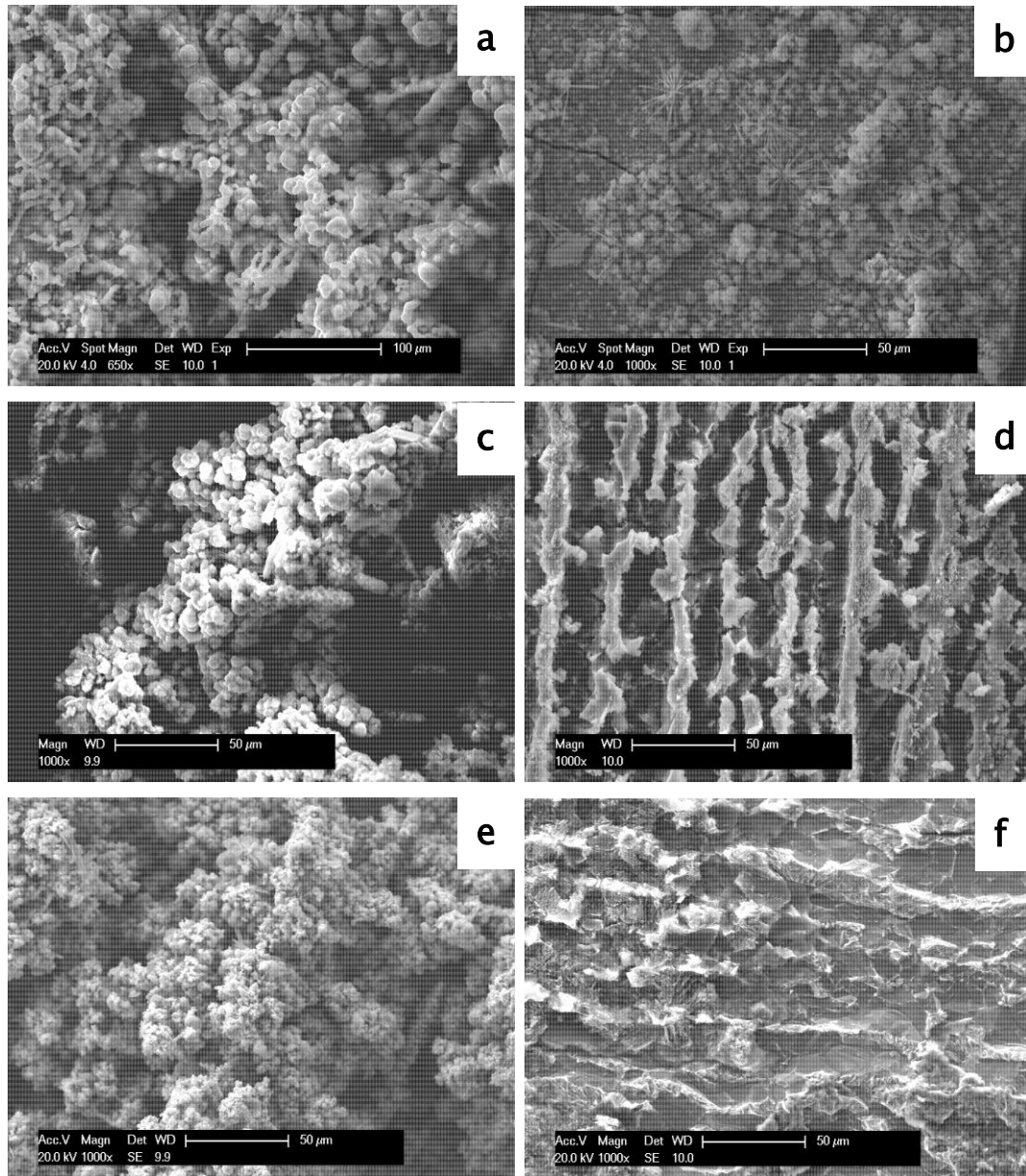


**Figure 3: Micrographs of (a) outer layer and (b) inner layer in 30 days, (c) outer layer and (d) inner layer in 90 days, (e) outer layer and (f) inner layer in 180 days of rust steels**

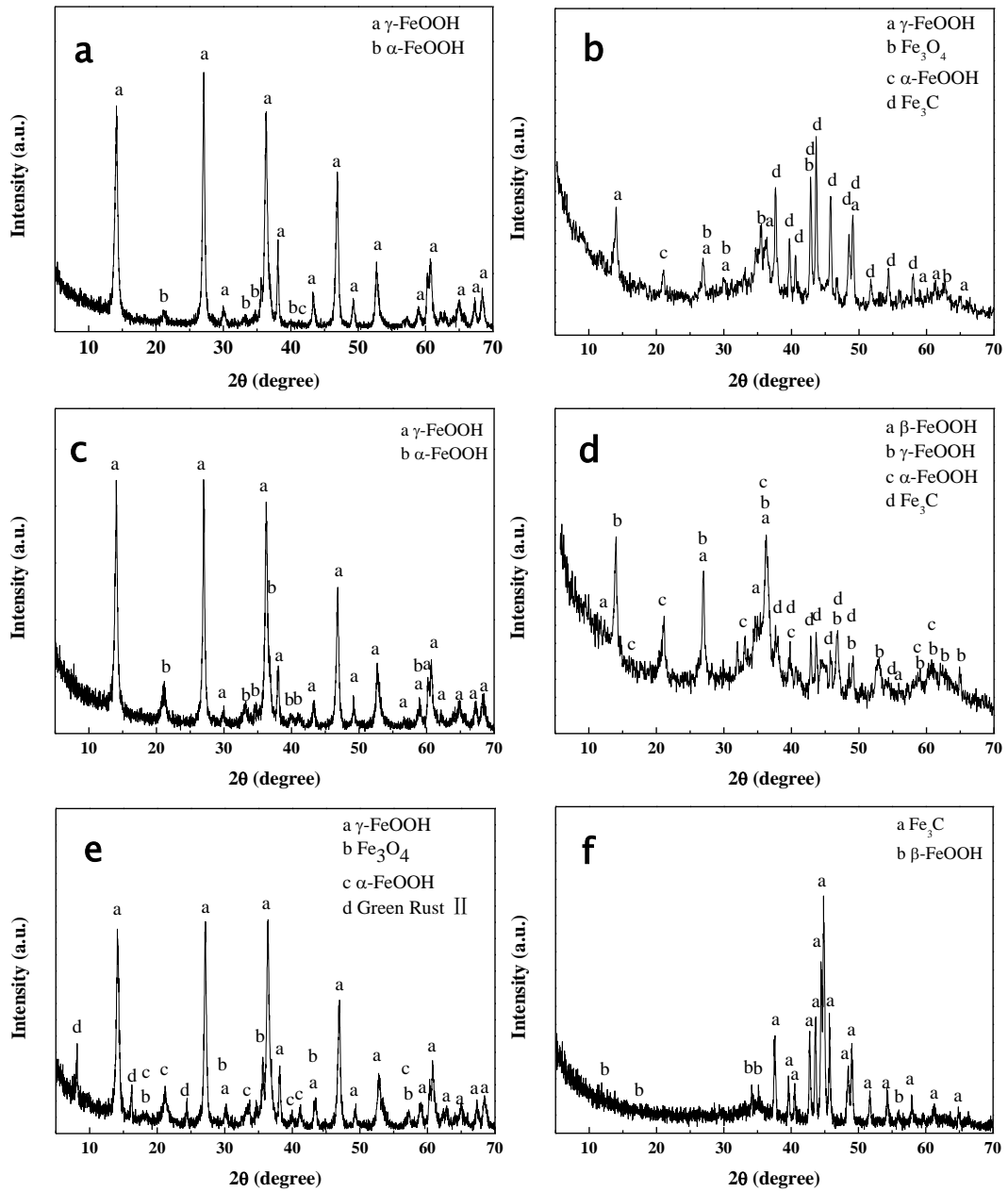


**Figure 4: XRD patterns of (a) outer layer and (b) inner layer in 30 days, (c) outer layer and (d) inner layer in 90 days, (e) outer layer and (f) inner layer in 180 days of DH36 rust steels**

From the SEM images and XRD results, the outer rust in 30 days was flaky, cluster distributed and not covered entire surface of the matrix. The main phase was  $\gamma$ -FeOOH with a small amount of  $\alpha$ -FeOOH. The inner rust layer is dense with cracks, and also with flaky and massive structures adhering. The rust covered almost the entire metal surface. The main ingredient was  $\text{Fe}_3\text{C}$  with a small amount of  $\gamma$ -FeOOH,  $\text{Fe}_3\text{O}_4$  and  $\alpha$ -FeOOH. The outer rust in 90 days was flaky, multilayer and only covered part of the metal surface. The

composition of the outer rust was same as that in 30 days. The inner rust layer was bent covered with strip distributed flaky structure. It was composed of  $\gamma$ -FeOOH,  $\text{Fe}_3\text{C}$ ,  $\alpha$ -FeOOH and  $\beta$ -FeOOH. The outer rust in 180 days was packing flaky but not dense. The rust composed of  $\gamma$ -FeOOH and a little of  $\text{Fe}_3\text{O}_4$  and  $\alpha$ -FeOOH. The presence of Green rust II was also observed. The inner rust was bent flaky with some cracks and composed of  $\text{Fe}_3\text{C}$  and a little of  $\beta$ -FeOOH.

## Discussion

The thickness of the rust layer increased with immersion time in seawater. The inner rust layer was bent flaky and composed of  $\text{Fe}_3\text{C}$  mainly. The outer layer was flaky with cracks and composed of  $\gamma$ -FeOOH and some  $\alpha$ -FeOOH. Large amount of  $\text{Fe}_3\text{C}$  was detected in inner rust, which was less reported in seawater corrosion.  $\text{Fe}_3\text{C}$  is not corrosion rusts in marine environment, and it is an originally presence in the steel. As the main carbon form,  $\text{Fe}_3\text{C}$  played the cathodic rule while iron anodic. With the metal dissolved, the carbon form left on the metal forming the inner layer. With the presence of  $\text{Fe}_3\text{C}$ , the rust was unable to form a protective layer, resulting in the increased corrosion rate in half a year.  $\beta$ -FeOOH is a typical rust in  $\text{Cl}^-$  contained environment, and it is loose and cannot protect the matrix. In addition, the  $\alpha$ -FeOOH in outer rust layer was obtained from  $\gamma$ -FeOOH with time.

## Conclusions

- (1) The inner layer of DH36 rust steel was bent flaky while the outer layer was packing flaky with cracks. The inner layer was composed of cementite mainly while the outer layer composed of lepidocrocite mainly.
- (2) The thickness of the outer layer increased with time in half a year while the inner rust was complex.
- (3) Lots of cementite was detected in inner rust and played cathodic zone. With the metal dissolved, cementite left on the metal and formed the inner layer. With the presence of cementite, no protective layer was formed, so it led to increasing corrosion rate in the test time.

## Acknowledgements

This work was funded by the Projects of National Natural Science Foundation of China (51301201) and Shandong Provincial Natural Science Foundation, China(ZR2013EMQ014).

## References

- [1] 'Influence of pitting and iron oxide formation during corrosion of carbon steel in unbuffered NaCl solutions', L. Cáceres, T. Vargas and L. Herrera, *Corrosion Science*, **51**, 5, pp 971–978, 2009.
- [2] 'Corrosion behavior of different alloys exposed to continuous flowing seawater by electrochemical impedance spectroscopy (EIS)', K. Al-Muhanna and K. Habib, *Desalination*, **250**, 1, pp 404–407, 2010.
- [3] 'Utilization of rice husk-bark ash to improve the corrosion resistance of concrete under 5-year exposure in a marine environment', W. Chalee, T. Sasakul, P. Suwanmaneechot and C. Jaturapitakkul, *Cement and Concrete Composites*, **37**, pp 47–53, 2013.
- [4] 'Outdoor-indoor corrosion of metals in tropical coastal atmospheres', F. Corvo, T. Perez, L. R. Dzib, Y. Martin, A. Castaneda, E. Gonzalez and J. Perez, *Corrosion Science*, **50**, 1, pp 220–230, 2008.
- [5] 'Long-term atmospheric corrosion of mild steel', D. de la Fuente, I. Díaz, J. Simancas, B. Chico and M. Morcillo, *Corrosion Science*, **53**, 2, pp 604–617, 2011.
- [6] 'Long-term corrosion of cast irons and steel in marine and atmospheric environments', R. E. Melchers, *Corrosion Science*, **68**, pp 186–194, 2013.
- [7] 'Statistical characterization of surfaces of corroded steel plates', R. E. Melchers, M. Ahammed, R. Jeffrey and G. Simundic, *Marine Structures*, **23**, 3, pp 274–287, 2010.
- [8] 'Atmospheric corrosion of Galfan coatings on steel in chloride-rich environments', X. Zhang, C. Leygraf and I. Odnevall Wallinder, *Corrosion Science*, **73**, pp 62–71, 2013.
- [9] 'Super-hydrophobic film prepared on zinc and its effect on corrosion in simulated marine atmosphere', P. Wang, D. Zhang, R. Qiu, J. Wu and Y. Wan, *Corrosion Science*, **69**, pp 23–30, 2013.
- [10] 'Splash zone protection on offshore platforms – A Norwegian operator's experience', R. E. Lye, *Materials Performance*, **40**, 4, pp 40–45, 2001.
- [11] 'Atmospheric corrosion of hot and cold rolled carbon steel under field exposure in Saudi Arabia', S. Syed, *Corrosion Science*, **50**, 6, pp 1779–1784, 2008.
- [12] 'Atmospheric corrosion of low carbon steel in a polar marine environment. Study of the effect of wind regime', S. Rivero, B. Chico, D. De la Fuente and M. Morcillo, *Revista De Metalurgia*, **43**, 5, pp 370–383, 2007.
- [13] 'Atmospheric corrosion of metals in regions of cold and extremely cold climate (a review)', A. Mikhailov, P. Strekalov and Y. Panchenko, *Protection of Metals*, **44**, 7, pp 644–659, 2008.



- [14] 'Characterization of pitting corrosion in bare and sol-gel coated aluminum 2024-T3 alloy', N. Voevodin, C. Jeffcoate, L. Simon, M. Khobaib and M. Donley, *Surface and Coatings Technology*, **140**, 1, pp 29–34, 2001.
- [15] 'Corrosion behavior of steel under wet and dry cycles containing  $\text{Cr}^{3+}$  ion', T. Kamimura, S. Nasu, T. Segi, T. Tazaki, S. Morimoto and H. Miyuki, *Corrosion Science*, **45**, 8, pp 1863–1879, 2003.
- [16] 'Corrosion of steel rebar embedded in natural pozzolan based mortars exposed to chlorides', G. Fajardo, P. Valdez and J. Pacheco, *Construction and Building Materials*, **23**, 2, pp 768–774, 2009.
- [17] 'Corrosion of vertical mild steel strips in seawater', R. Jeffrey and R. E. Melchers, *Corrosion Science*, **51**, 10, pp 2291–2297, 2009.
- [18] 'Corrosion product formation during NaCl induced atmospheric corrosion of magnesium alloy AZ91D', M. Jönsson, D. Persson and D. Thierry, *Corrosion Science*, **49**, 3, pp 1540–1558, 2007.
- [19] 'Corrosion of copper in seawater and its aerosols in a tropical island', L. Nunez, E. Reguera, F. Corvo, E. Gonzalez and C. Vazquez, *Corrosion Science*, **47**, 2, pp 461–484, 2005.
- [20] 'Characterization of the rust formed on weathering steel exposed to Qinghai salt lake atmosphere', Q. X. Li, Z. Y. Wang, W. Han and E. H. Han, *Corrosion Science*, **50**, 2, pp 365–371, 2008.
- [21] 'The effect of  $\beta\text{-FeOOH}$  on the corrosion behavior of low carbon steel exposed in tropic marine environment', Y. Ma, Y. Li and F. Wang, *Materials Chemistry And Physics*, **112**, 3, pp 844–852, 2008.
- [22] 'Corrosion of low carbon steel in atmospheric environments of different chloride content', Y. T. Ma, Y. Li and F. H. Wang, *Corrosion Science*, **51**, 5, pp 997–1006, 2009.
- [23] 'Atmospheric corrosion of carbon steel in Colombia', J. G. Castaño, C. A. Botero, A. H. Restrepo, E. A. Agudelo, E. Correa and F. Echeverría, *Corrosion Science*, **52**, 1, pp 216–223, 2010.
- [24] 'Characterization of Corrosion Products on Carbon Steel Exposed to Natural Weathering and to Accelerated Corrosion Tests', R. A. Antunes, R. U. Ichikawa, L. G. Martinez and I. Costa, *International Journal of Corrosion*, **2014**, pp 9, 2014.
- [25] 'Corrosion resistance and mechanical properties of low-alloy steels under atmospheric conditions', Y. Y. Chen, H. J. Tzeng, L. I. Wei, L. H. Wang, J. C. Oung and H. C. Shih, *Corrosion Science*, **47**, 4, pp 1001–1021, 2005.
- [26] 'Characterization of High-Temperature Oxide Films on Stainless Steels by Electrochemical-Impedance Spectroscopy', J. Pan, C. Leygraf, R. F. A. J.-P. tersson and J. LindeÅn, *Oxidation Of Metals*, **50**, pp 431–455, 1998.